Materials Advances

ROYAL SOCIETY OF CHEMISTRY

PAPER

View Article Online
View Journal | View Issue

Cite this: *Mater. Adv.*, 2024, 5, 6873

Conductive MXene nanosheets infused in protein fiber hydrogels for bioprinting and thin film electrodes†

Mario Alfonso Arenas García,[a] Slah Hidouri,[a] Joshua M. Little,[b] Daniel Modafferi,[a] Xinxin Hao,[a] Po-Yen Chen[b] and Noémie-Manuelle Dorval Courchesne*[a]

Conductive hydrogels are materials of choice for wearable sensors and soft electronics. They are typically engineered by incorporating a conductive filler into a hydrophilic polymer network. MXene ($Ti_3C_2T_x$) is a remarkable 2D nanomaterial that can be used as a conductive filler with excellent electrical conductivity and high hydrophilicity. However, it has a poor self-supporting organization due to a lack of interactions between the nanosheets. To offset this problem, we used a biological scaffold composed of curli fibers to load conductive MXene nanosheets. Curli fibers are bacterial amyloid fibers that exhibit robust mechanical properties and have been shown to interact with a range of surfaces and nanomaterials. By varying the loading of MXene in curli-MXene nanocomposites (CMXn), we were able to modulate their conductivity and mechanical properties. At the lowest loading (25 wt%), we achieved a conductivity of 44 nS cm^{-1} with the films able to withstand a strain of up to 84%, in contrast to the highest loading (70 wt%) which reached a considerably higher conductivity of 49 S cm^{-1} but a strain at break of only 7%. All CMXn hydrogels exhibited shear thinning behavior and G'/G'' ratios between 2–5, suitable properties for extrusion printing. We conducted shelf-life studies over a month for the highest performing nanocomposite, identifying that storage temperatures had an impact on their conductivity as they retain 36% of its original conductivity when stored at 4 °C but lost 99% when left at room temperature. Overall, fabricating CMXn hydrogels capitalized on the self-assembly of curli fibers and their ability to form hydrogels suitable for bioprinting. By modulating the content of MXene in CMXn hydrogels, we tuned their conductivity and mechanical properties, which could suit different needs for sensing and soft electronic applications.

Received 4th February 2024,
Accepted 22nd July 2024

DOI: 10.1039/d4ma00112e

rsc.li/materials-advances

Introduction

Wearable sensors have been gaining traction in recent years, with a potential market worth of $25 billion USD by 2025.[1] Such devices have been fabricated to detect different biophysical and biochemical signals to obtain physiological information.[2] Conductive hydrogels are materials of choice that are considered for such applications, which not only include wearable pressure, strain or enzymatic sensors, but can also be used in soft electronics, artificial electronic skins, among others.[2,3] Hydrogels, which are 3-D hydrophilic polymer networks, typically show good biocompatibility and biodegradability, exhibit water retention capabilities, and mimic the elasticity, stiffness & permeability of the extracellular matrix.[3,4] To engineer conductive hydrogels that can interface living systems and electronic devices with varying degrees of conductivity, conductive fillers can be incorporated. This can be done by incorporating a suspension of a filler nanomaterial, by polymerizing a conductive material within a pre-formed hydrogel matrix, or by cross-linking conductive polymers with dopant molecules.[5] The main challenge is to achieve a high degree of conductivity without negatively impacting the mechanical properties of the hydrogels. Different matrices have been used in conductive hydrogels, such as chitosan, polyacrylamide (PAM) and polyvinyl alcohol (PVA), along with conductive fillers like PEDOT:PSS or polypyrrole (PPy), where concentrations of the matrix and conductive filler are finely tuned to achieve the desired properties.[3] However, polymers like PPy need to have their morphology altered to obtain their desired properties, and others, such as PEDOT, must be mixed with another component (such as PSS) in order to increase their solubility at the expense of conductivity.[6,7]

[a] Department of Chemical Engineering, McGill University, 3610 University Street, Montréal, QC, H3A 0C5, Canada. E-mail: noemie.dorvalcourchesne@mcgill.ca
[b] Department of Chemical and Biomolecular Engineering, University of Maryland, 4418 Stadium Drive, College Park, MD, 20742, USA

† Electronic supplementary information (ESI) available. See DOI: https://doi.org/10.1039/d4ma00112e

These additional steps make the use of some of these conductive fillers more complex, a drawback that can be addressed by using MXene as a conductive filler, directly without further modifications.

MXene is a type of 2D nanomaterial with a general chemical formula of $M_{n+1}X_nT_x$, where M is an early transition metal (Ti, Nb, Mo, among others), X is carbon and/or nitrogen and T_x represents the surface terminations (–OH, –O and –F).[8] MXene is synthesized by removing element A (from group IIIA or IVA) from $M_{n+1}AX_n$ phases, by exfoliating with HCL and LiF due to weak bonds and subsequent sonication in water results in the delamination of multilayered MXene sheets.[9] MXene nanosheets show promising properties as conductive fillers due to their high electrical and thermal conductivities, with reported values reaching up to 2.4×10^5 S m^{-1} and 2.84 W m^{-1} K^{-1} respectively as well as high capacitance, hydrophilicity, antimicrobial properties and ease of synthesis.[8,10–13] However, MXene suffers from poor self-supporting organization due to the lack of interlayer interactions between the nanosheets, which makes it difficult to process this material by itself to fabricate free-standing self-supported electrodes.[14] To overcome this limitation, MXene has been previously mixed with a variety of polymers such as PVA, polyurethane or polyaniline or coated on textile surfaces in order to be used in a variety of applications such as epidermal sensors, bone scaffolds as well as in stretchable devices and self-healing conductive hydrogels.[15–17] MXene has notably been used in a variety of stretchable devices with some issues encountered, including a loss of ability to form fibers, a reduction in stretchability depending on the content of MXene in the composite, as well as difficulties in integrating or coating surfaces with MXene. In addition, these existing composites are generally not biodegradable.[17]

To address some of these processability challenges, we propose using a biological matrix, curli fibers, to form a biocomposite with MXene. Curli fibers are an important component of the extracellular matrix in biofilms produced by a variety of *Enterobacteriaceae*.[18] Given their role in the formation of biofilms, curli fibers can adhere to a variety of surfaces (such as stainless steel or Teflon), facilitating their interaction with a range of nanomaterials.[19] Curli fibers could thus facilitate the binding, dispersion and loading of MXene within a hydrogel. The high water content of curli fibers in their hydrogel form would also be compatible with the hydrophilic nature of MXene.[18] Additionally, curli fibers can be isolated from bacterial biofilms through a simple, fast and established vacuum filtration protocol which can yield hundreds of milligrams of protein fibers per liter of bacterial culture.[20] A different steps of this vacuum filtration process, nanomaterials like MXene may be integrated to infuse curli fiber hydrogels, to generate biocomposites in a scalable manner.

Curli fibers have been previously used to produce a variety of different plastic-like materials and composites. For instance, they have been used to fabricate thin films that were called ''aquaplastics'', by allowing the fibers to gel in the presence of a surfactant during their isolation from bacterial cultures.[21] ''Aquaplastics'' were processed under ambient conditions, in contrast to traditional thermoplastics. They exhibited a biodegradation rate comparable with nanocellulose under aerobic conditions and displayed self-healing in the presence of water, a property that could also be exploited to weld different films together. The latter property was also taken advantage of in the formation of PEDOT:PSS thin film composites. In these materials, the curli fibers could also be used to tune the Young's modulus, and they could be genetically engineered to display other important features such as surface adhesion and improved conductivity through aromatic residues.[19,22–24] When mixed with PEDOT:PSS, curli fibers modified the microstructure of the films but also enabled the films to self-heal faster and provided conductivity enhancement at an optimal loading ratio.[22] Curli fibers also exhibit shear thinning properties, which have allowed them to be used for 3D printing purposes.[25] Together, the ability of curli fibers to self-heal, to be extruded and to modulate the mechanics of composites, makes them scaffolds of interest for processing composites with different methods including wet or dry spinning as well as simple extrusion printing.

In this work, we loaded MXene nanosheets into curli fibers to fabricate conductive hydrogels while guaranteeing a self-supporting structure enabled by the curli matrix. The resulting mechanical properties allowed us to use the curli-MXene nanocomposites (CMXn) as hydrogels for printing or as conductive thin films. MXene was incorporated during the isolation of curli fibers from bacterial biofilms *via* a simple vacuum filtration process. After optimizing the loading of the nanosheets into curli hydrogel and assessing the homogeneity of MXene in the nanocomposite, the loading of MXene was varied. Afterwards, the mechanical properties were assessed and the conductivity of the nanocomposites, both of which were found to depend on the MXene loading. Thus, incorporating MXene within curli hydrogels with different ratios enables the fabrication of CMXn hydrogels with tunable properties.

Experimental

Materials

Titanium aluminum carbide (Ti_3AlC_2, MAX phase) was purchased from Tongrun Info Technology Co. Ltd (Luoyang, China). Lithium fluoride (LiF), Fisherbrand Plain Glass Microslides, acetone (certified ACS) and 2-propanol (ACS grade) were obtained from Fisher Scientific (Ottawa, Canada). Hydrochloric acid (HCl) was purchased from ACP Chemicals (St. Leonard, Canada). Lysogeny broth (LB) agar media, D-glucose, carbenicillin, guanidinium chloride (GdmCl), sodium dodecyl sulphate (SDS) electrophoresis grade and glycerol 99.5% were purchased from BioShop Canada Inc. (Burlington, Canada). Benzonase nuclease was purchased from Millipore Sigma (Oakville, Canada). Polypropylene/polyethylene filters with 10 μm pore size were purchased from Pall Corporation (Mississuauga, Canada). Glutaraldehyde 50% solution was purchased from BioBasic Inc. (Markham, Canada). Paraformaldehyde 16% and sodium cacodylate buffer 0.4 M, pH 7.2 were purchased

from Electron Microscopy Sciences (Hatfield, United States). Silver-based ink Voltera Conductor 2 was purchased from Voltera (Waterloo, Canada).

Synthesis of MXene

The synthesis of MXene was performed following an established protocol.[9] In an oil bath at 35 °C, 3 g of LiF were slowly added to a container with 40 mL of a 9 M HCl solution. Mixing was done with a magnetic stirrer bar. One gram of Ti_3AlC_2 was progressively added to avoid a strong exothermic reaction. The solution was then left agitating at 330 rpm for 24 hours and allowed to vent. The resulting solution was then split between two 50 mL centrifuge tubes which were filled with cold 2 M HCl solutions up to the 45 mL mark. The tubes were then centrifuged at 4000 rpm for 15 min. The supernatant was decanted, and this process was repeated two more times. The solution was then washed with deionized (DI) water by filling the centrifuge tubes up to the 45 mL mark and then agitated and vortexed before centrifuging at 4000 rpm for 15 min. This was repeated until the supernatant approximately reached pH 5. At that point, a 10 min sonication step was employed to delaminate the stacked MXene layers. Lastly, the solutions were then centrifuged at 4000 rpm for 30 min and the supernatant was collected, wrapped in aluminum foil and stored at 4 °C.

Production, isolation of curli fiber hydrogels and loading with MXene

The *Escherichia coli* (*E. coli*) mutant strain PQN4, from which the native curli operon has been removed, and the plasmid pET21d-*csgACEFG* which contains a T7 promotor for inducible curli expression were gifted by the Joshi Lab (Harvard University, Boston, MA).

Electrocompetent *E. coli* PQN4 cells were transformed with pET21d-*csgACEFG* plasmid and then streaked onto LB agar plates that contained 100 μg mL^{-1} carbenicillin and 2% (w/v) glucose. The plates were incubated overnight at 37 °C. A colony was picked and grown overnight in 5 mL LB media with 100 μg mL^{-1} carbenicillin and 2% glucose, at 37 °C and 225 rpm. The overnight culture was then added to 500 mL of LB media that containing 100 μg mL^{-1} of carbenicillin. The large scale was grown for 30 hours at 37 °C and 225 rpm.

Curli fibers were then isolated *via* an established vacuum filtration method.[20] The culture was incubated with GdmCl at a final concentration of 0.8 M for 30 min at 4 °C. The culture was then vacuum filtered with 10 μm pore sized polypropylene/polyethylene membranes until the filters were clogged. The medium was then incubated with 5 mL of 8 M GdmCl for 5 min, followed by vacuum filtration and multiple washes with DI water. Remaining nucleic acids were degraded by incubating with Benzonase nuclease (1.5 U mL^{-1}) for 10 min and then vacuum filtered and washed several times with DI water. Thereafter, to promote gelation and delaminate the protein fibers, they were incubated with 5% SDS for 5 min, vacuum filtered and washed thoroughly with DI water.

The incorporation of MXene in the vacuum filtration process was assessed at three stages: (1) adding MXene to curli fibers before gelation, (2) adding MXene during the gelation of curli fibers and lastly, (3) adding MXene after their gelation. After determining that the most advantageous incorporation method was before the gelation of curli fibers, different concentrations of aqueous MXene dispersions were incubated (1 mg mL^{-1}, 2 mg mL^{-1}, 3 mg mL^{-1} & 4 mg mL^{-1}) for a period of 10 min, followed by vacuum filtration and multiple washes with DI water.[21] Finally, CMXn hydrogels were removed from the filter with a spatula and stored at 4 °C and wrapped in aluminum foil until needed.

Curli-MXene nanocomposite films were generated by mixing CMXn hydrogels with 50% (w/v) glycerol to a final concentration of 2% (w/v) and 500 μL were deposited in a 20 mm × 5 mm × 3 mm silicon mold. They were left drying for a period of 48 h and were retrieved afterwards for further measurements.

Dried samples were prepared for characterization. For comparison, MXene and CMXn hydrogel samples were stored at −80 °C and then lyophilized for 4–8 h at 0.210 Torr and −55 °C. The samples were then made into powder for XRD, FTIR spectroscopy and TGA.

X-ray diffraction

X-ray diffraction (XRD) scan was recorded from 20 to 80 degrees (2θ), with increments of 0.5 degrees and this analysis was conducted using a Bruker D8 Advance X-ray diffractometer equipped with a Cu Kα source (λ = 1.5418 nm).

Fourier transform-infrared spectroscopy

Fourier transform-infrared (FTIR) spectroscopy was used in attenuated total reflectance (ATR) mode. The spectra ranged from 4000 to 550 cm^{-1} with a resolution of 2 cm^{-1} and an average of 64 scans. These analyses were performed using a spectrometer Alpha II from Bruker.

Thermogravimetric analysis

Thermogravimetric analysis (TGA) experiments were done using a TA Instruments TGA 5500 device. Samples (between 3–10 mg) were run at 20 °C min^{-1} up to a temperature of 800 °C under a nitrogen stream of 25 mL min^{-1} in alumina pans. The MXene loading content was calculated using eqn (1).

$$\mathrm{CMXn_f\ wt\%} - \mathrm{curli\ fibers_f\ wt\%} + (\mathrm{MXene_f\ wt\%} - \mathrm{MXene_i\ wt\%}) \quad (1)$$

Scanning electron microscopy and elemental mapping

Curli-MXene nanocomposites were imaged by filtering 30 μL of CMXn hydrogels onto a polycarbonate hydrophilic 0.2 μm pore track-etch filter membranes (Whatman). The samples were then fixed with 2% (w/v) glutaraldehyde, 2% (w/v) paraformaldehyde and 0.1 M sodium cacodylate for 2 h at RT. Afterwards, the samples were washed with DI water for 15 min and then with increasing concentrations of ethanol (25%, 50%, 75% and 100% v/v) for 15 min each. The fixed composite material was then dried using a critical point drier, and sputter coated with platinum to a thickness of 4 nm. SEM imaging of the samples was done using a FEI Quanta 450 Environmental Scanning

Electron Microscope and elemental mapping through EDS was done using an EDAX Octane Super 60 mm^2 SDD and TEAM EDS Analysis System.

Rheological measurements of CMXn hydrogels

The rheological properties of the CMXn hydrogels were measured using an Anton Paar MCR 302 rheometer with a disposable 25 mm flat plate. All measurements were done at room temperature. The nanocomposites were loaded and excess along the edge was trimmed. Shear thinning behavior was investigated by measuring shear viscosity under a continuous flow at shear rates from 0.01–100 s^{-1}. To determine the storage (G') and loss (G'') modulus, the samples were subjected to an oscillatory strain sweep from 0.01 to 1000% at a constant frequency of 0.1 Hz as well as under an oscillatory shear strain of 0.5% with the frequency increasing from 0.1 to 100 Hz.

Tensile tests for CMXn films

The stress–strain curves of the CMXn films were determined using a mechanical testing machine (Instron 68SC-05) fitted with a 500-N load cell. After calibrating the load cell, the CMXn films were cut into 2 cm long × 1 cm wide strips and subject to a tensile test at an extension rate of 5 mm min^{-1}. The tensile tests started with an initial fixture gap of 1 cm. Three measurements were conducted for each CMXn film. The thickness of the CMXn films were estimated be between 50–100 μm.

Electrode fabrication

Glass slides were cleaned by submerging and sonicating subsequently in DI water with soap, acetone, and isopropanol for 5 min each. The slides were washed thoroughly with DI water after sonicating with soapy DI water. The electrodes were printed with silver-based ink Voltera Conductor 2 (Voltera) using a Voltera V-One PCB Printer. The electrodes were designed to have a spacing of 2 mm and to be 3 mm long. A window was made using scotch tape to facilitate the casting of the composite hydrogel and to avoid any leaks between the electrodes.

Printing CMXn hydrogels and electrical characterization

The CMXn hydrogels were loaded into a 0.3 mL syringe with a 31 G × 6 mm needle which then extruded five lines with a length of 5 mm onto a clean glass slide. Afterwards, the printed samples were left drying for at least 1 hour at RT and 45% RH.

Tungsten tips were connected to the printed CMXn lines. Using an Agilent B1500A semiconductor device analyzer, *I–V* sweeps (from −500 to 500 mV) were run on all samples at RT and 45% RH. The thickness (d) and width (w) of the printed lines were measured using a Dektak XT profilometer with a 12.5 μm tip and a 3 mg stylus force. The thickness of the printed CMXn lines were on average between 10–30 μm while their width was between 1.0–1.5 mm. The conductivity (σ) of the lines were calculated using eqn (2), where G = conductance and l = line length.[22]

$$\sigma = G\frac{l}{wd} \quad (2)$$

To determine the shelf life of the conductive CMXn hydrogel and aqueous MXene dispersion, a CMXn hydrogel sample with MXene loading of 70 wt% along with a MXene dispersion of 4 mg mL^{-1} was assessed under different conditions, one left inside the fridge at 4 °C and covered in aluminum foil and another left at RT with no aluminum wrapping.

From each storage condition, five lines of CMXn-70 were printed on a clean glass slide along with 2 μL of the MXene dispersion casted onto five silver printed electrodes. These were printed every four days and were measured with the aforementioned method until 32 days passed. The stability of the printed CMXn-70 hydrogel lines were also assessed and measured for the same time span.

Results & discussion

Fabrication of CMXn hydrogels

First, we sought to determine the best method for incorporating MXene nanosheets within curli fiber hydrogels prepared *via* vacuum filtration, a well-established protocol for isolating curli fibers as previously described.[20] During this process, curli fibers expressed from a liquid bacterial culture are isolated based on their size, washed to remove impurities and treated with a surfactant (sodium dodecyl sulfate (SDS)), which has a gelation effect and enables delamination of the protein fibers from the filter membrane. We hypothesized that MXene would interact or diffuse differently within the curli fiber hydrogel depending on the incorporation methods, and opted for adding an aqueous dispersion of MXene at a concentration of 4 mg mL^{-1} at three different steps of the process (Fig. 1(a), shown with stars): (1) addition of MXene to the curli fibers before gelation to allow for interactions between the materials; (2) addition of MXene during the gelation of the curli fibers; (3) addition of MXene after the gelation.

The performance of these methods was compared by printing CMXn hydrogels and measuring their conductivity as a metric, and obtained the best performance from MXene added pre-gelation, with a conductivity of 590 ± 70 mS cm^{-1}. In comparison, when MXene was added during or post-gelation, the resulting conductivities were 1.2 ± 0.6 μS cm^{-1} and 60 ± 30 nS cm^{-1} respectively (see Fig. 1(b)). These large differences were attributed to the varying load of MXene incorporated into CMXn hydrogels, as measured with thermogravimetric analysis (TGA) (Fig. S1c, in ESI†). A MXene load of 38 wt% was achieved when MXene was allowed to interact with curli fibers in the culture medium prior to vacuum filtration, while the load of MXene did not surpass 17–19 wt% when it was incorporated during or post-gelation, after curli fibers were initially collected on a filter membrane (Fig. 1(b) and Fig. S1c, ESI†). We postulate that, when incorporated in the liquid culture, MXene is allowed to interact with curli fibers *via* electrostatic interactions, while it may be difficult for the nanosheets to completely diffuse through the curli fiber gel (given that they form nanometric pores) when incorporated during or post-gelation.[20] In addition, we also noticed the formation of aggregates after 2–3 h

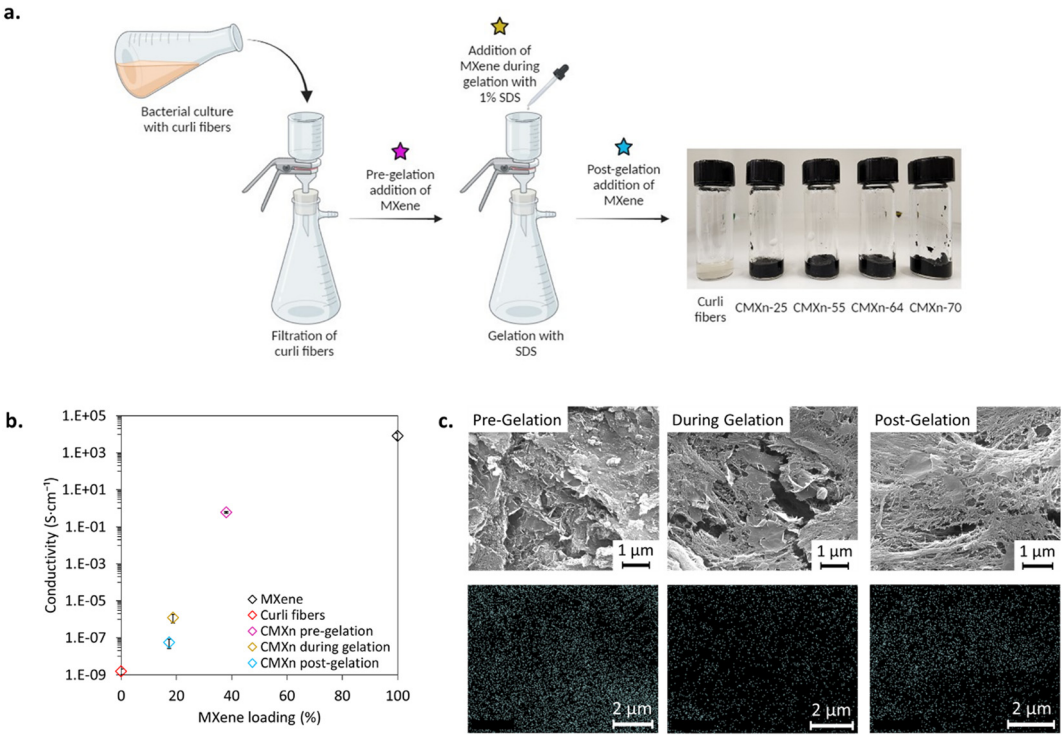

Fig. 1 The integration of MXene at different stages results in CMXn hydrogels with different morphologies and conductivities. (a) Schematic of the fabrication of CMXn hydrogels and photographs of nanocomposites with increasing MXene loadings. The stars indicate three stages in the vacuum filtration procedure at which the integration of MXene with curli fibers was studied. The numbers labelled on CMXn hydrogels indicate their MXene loading content in wt%. (b) Conductivity measurements of CMXn hydrogels for the integration of aqueous MXene dispersion at different stages, and (c) corresponding SEM images and EDS elemental mapping for Ti.

when MXene is mixed with SDS, which could indicate interactions between MXene and SDS, and lead to reduced interactions between MXene and curli fibers. Such an effect has been reported when assessing SDS on the oxidation impact of MXene.[26]

The differences in the morphology of CMXn hydrogels fabricated with different methods were visually assessed *via* scanning electron microscopy (SEM) and elemental mapping through energy-dispersive X-ray spectroscopy (EDS). We mapped the presence of titanium (Ti) as a marker for MXene and noticed a weaker signal from the CMXn hydrogel prepared during gelation in contrast to CMXn hydrogels where MXene was added pre- or post-gelation (Fig. 1(c)). However, CMXn hydrogel pre-gelation displayed better conductivity and possessed a higher MXene loading. The apparent stronger signal from CMXn hydrogel prepared post-gelation may be due to the fact that the sample thicknesses were not controlled for the purpose of SEM imaging and EDX mapping. The SEM images also revealed differences in morphology of the nanocomposites, with a structure exhibiting more flake-like features for MXene incorporated in liquid culture and thus at a higher concentration, and a more fibrous structure when curli fibers dominate in content.

Taken together, these results indicate that MXene can be more efficiently incorporated within the nanocomposites when it is allowed to first interact with curli fibers pre-gelation, producing a more homogeneous material with a greater MXene load and thus a higher conductivity. Hence, subsequent experiments proceeded with this fabrication method.

Characterization of CMXn hydrogels

First, a method based on TGA was established to correlate the concentration of MXene used during the integration with curli fiber hydrogels with the final MXene loading in the CMXn hydrogels (Fig. 2(a)). This method also allowed us to assess if the different dispersions of MXene would reproducibly result in the same loading of MXene. To do so, three batches of CMXn hydrogels were produced for each concentration of MXene dispersion used and then determined the MXene loading using TGA, taking advantage of the different thermal stabilities of curli and MXene, as seen in Fig. 2(a). The decomposition curves show that curli fibers have four main stages for their weight loss, losing 3 wt% starting from room temperature (RT) up to 160 °C which is attributed to water. The second stage lasts up to 280 °C and losing 32 wt%, the third stage up to 630 °C with a weight loss of 36% while and the final stage up to 800 °C. The majority of the mass occurs between 200–400 °C, which attributed to the of the polypeptide bonds through deamination, decarboxylation and depolymerization.[27] Curli fibers decompose entirely by 800 °C, however, there are likely trace minerals present in the curli fibers which may correspond to the residues of guanidinium chloride (GdmCl) and SDS as well as ash, comprising a remaining 13 wt% of the weight beyond this temperature. Pure MXene, on the other hand, displays two

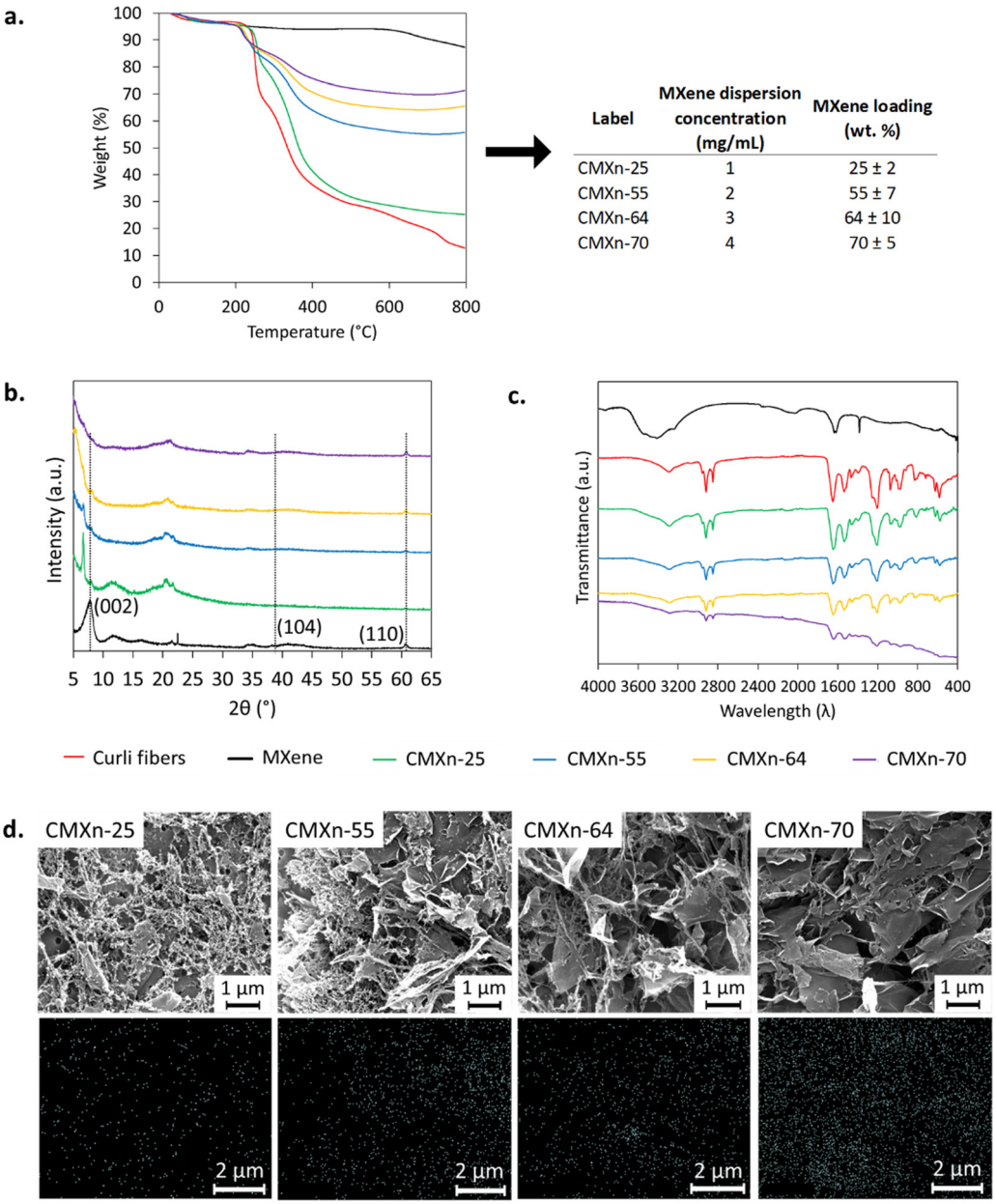

Fig. 2 MXene loading in CMXn hydrogels varies with the concentrations of MXene dispersions ranging from 1 to 4 mg mL^{-1}, after incubation with curli fibers. Assessment of the loading through (a) TGA with table that correlates MXene dispersions used and their corresponding loading weights in CMXn hydrogels. The nanocomposites were labelled according to their MXene loading content, (b) XRD, (c) FTIR spectroscopy, and (d) SEM images of CMXn hydrogels with corresponding EDS elemental mapping for Ti.

stages of degradation. The first stage is from RT until 500 °C losing 5.8 wt% which may be attributed to trapped structural water while the second stage lasts until 800 °C, where it loses 6.8 wt% and may be due to a dissociation of surface groups.[28] The overall loss is greater than what has been reported, with values ranging from 2–10 wt%.[28,29] Lastly, the CMXn hydrogels show three main stages for their weight loss, starting from RT up to 150 °C, the second stage up to 280 °C and the third stage up to 800 °C; a similar behavior reported to that of MXene–PVA blends.[30] The weight loss is similar in the first two stages among all CMXn hydrogels, ranging from 3–5 wt% for the first stage and 12–18 wt% for the second stage. The final stage changes notably among all the concentrations, with CMXn-25 showing a drop of 54 wt%, CMXn-55 showing a drop of 28 wt%, CMXn-64 showing a drop of 21 wt% and CMXn-70 showing a drop of 16 wt%. Thermogravimetric data shows that there was a substantial increase in the loading of MXene when increasing the concentration of the MXene dispersion from 1 mg mL^{-1} to 2 mg mL^{-1} for CMXn-25 to CMXn-55 (an approximate 2-fold increase), and that the loading would then plateau when using MXene dispersion of 3–4 mg mL^{-1} (for CMXn-64 and CMXn-70).

We then proceeded to evaluate how different MXene loading contents would affect the properties of CMXn hydrogels, as this is directly correlated to its conductivity. To do so, curli fibers were incubated with different concentrations of aqueous MXene dispersions (from 1 to 4 mg mL^{-1}), reasoning that by doing so the amount of MXene interacting with curli fibers would increase. The interactions of MXene with curli fibers in the nanocomposites (Fig. 2(b) and (c)) was then assessed through X-ray diffraction (XRD) and Fourier transform-infrared (FTIR) spectroscopy to determine if there were any changes in the structure of MXene and/or curli fibers.

Given that MXene was originally synthesized from MAX phase, it was also important to establish if the synthesis of MXene was successful. The XRD patterns of MXene and associated materials were obtained, as shown in Fig. 2(b). A decrease was observed in the peak situated near $2\theta = 40^\circ$ and attributed to *hkl* plane (104), which is characteristic for Ti_3AlC_2 (MAX phase), along with a reduction and a shift of the peak of $2\theta = 7.9^\circ$ attributed to (002) and a peak near 61° attributed to (110) *hkl* plane.[29,31,32] The reduction of the (002) peak shows that the MXene sheets are no longer stacked.

Then, we compared pure MXene with CMXn hydrogels. First, in CMXn hydrogels, the increasing MXene load could be tracked *via* the (110) peak which increased in intensity. We also observed shifts and broadening of certain peaks in CMXn hydrogels. First, the XRD pattern revealed that the (002) peak shifted towards lower angles $2\theta \approx 5^\circ$. Such trends were also observed previously when MXene was blended with other polymers like PVA and PAM.[10,30,32,33]

We then verified whether interactions between curli fibers and MXene would be detectable through FTIR analysis (Fig. 2(c)). The spectra of MXene showed a similar behavior to previously published results, displaying a peak at approximately 3400 for –OH as well as near 1600 for –C═O.[26] There is also a peak near 1400 which is attributed to –OH.[34] However, the spectra did not show any peak shifts or the appearance of new bonds. As expected, the results simply confirmed the relative MXene and curli fiber content changes within the nanocomposites. The results showed that peaks for –OH groups (3500–3200 cm^{-1} band), amide I (1690–1600 cm^{-1}), amide II (1575–1480 cm^{-1}) and characteristic amyloid peaks near 2750 cm^{-1} & 1200 cm^{-1} all decreased as the content of MXene increased in the nanocomposites.[24] The surface groups present in MXene are largely dependent on the procedure used to delaminate the layers.[35] Etching with HCl/LiF results in the formation of –OH, ═O and –F terminated groups on the surface of MXene.[9,36,37] Additionally, MXene has a negative surface charge at pH from 4–10.[38] On the other hand, curli fibers primarily display polar groups on their β-helical surface, such as asparagine, serine, glutamine and threonine.[39] We postulate that these groups primarily interact with MXene through their hydrophilic nature.[8] At pHs around 4–5, which is expected for curli fibers obtained after vacuum filtration, curli fibers exhibit a neutral to slightly positive net surface charge. Thus, positively charged hydrophilic residues on curli could establish electrostatic interactions with negatively charged MXene nanosheets.

Lastly, a uniform distribution of MXene in CMXn hydrogels is desired, as this can have an impact on the conductivity of the nanocomposite. The homogeneity of CMXn hydrogels was assessed through SEM imagery (Fig. 2(d)) and observed that at lower MXene loadings, curli fibers completely envelop MXene sheets, as seen for CMXn-25 and CMXn-55. This contrasts with what is seen with CMXn-64 and CMXn-70, in which a greater coverage of MXene sheets is observed. The envelopment of MXene sheets by curli fibers seen at lower MXene loading may also explain the lower conductivity measured for CMXn-25 and CMXn-55, given that the protein is acting as an insulator between the MXene sheets and not only as a scaffold. We also mapped the presence of Ti as a marker for MXene and confirmed that the signal increased in intensity as the loading of MXene increased in CMXn hydrogels.

Mechanical properties of curli-MXene nanocomposite

We evaluated the rheological properties of CMXn hydrogels to determine their potential usage as an extrudable conductive bioink. All CMXn hydrogels exhibited shear thinning properties (Fig. 3(b)), which is an ideal feature for printing purposes. Curli fibers have an approximate viscosity of 25 Pa s which decreases as the shear rate increases, a similar behavior reported by Huyer *et al.* (2022) at RT. The viscosity of CMXn-25 is very similar to that of curli fibers, due to its low MXene loading. There is a noticeable difference in viscosity with CMXn-55, -64 and -70. The behavior exhibited by the CMXn hydrogels with higher MXene loading is very similar to that of another report which notes that as MXene loading increases, then the viscosity increases, with the final value also depending on the number of layers present in the MXene nanosheets.[8] The changes in viscosity in the CMXn hydrogels can be particularly important as this parameter could be tuned depending on the desired extrusion device in a printing process.

The storage (G') and loss (G'') modulus were also investigated to assess the stability and behavior of CMXn hydrogels (Fig. 3(c) and (d)). Amplitude sweeps (Fig. 3(c)) showed that curli fibers and all CMXn hydrogels had a linear viscoelastic region (LVE) until an approximate strain of 2% while showing that G' was larger than G'', which indicated gel-like behavior. Above this value, their G' decreased as G'' increased and had a crossover. The drop in the LVE region is slightly in contrast with previously reported values for curli fibers (10% strain), a difference that may be attributed due to the use of different engineered curli fibers in previous reports as opposed to wild-type fibers here.[25] On the other hand, the addition of MXene did not result in a modification of the LVE region but did increase the G' and G'' of CMXn hydrogels.

CMXn-70 showed significant differences when compared to the rest of the nanocomposites. Frequency sweeps of CMXn-70 showed that the G' modulus was 5-fold larger than the G'' modulus of CMXn-70, while the remaining nanocomposites as well as curli fibers only displayed a 2-fold difference. By calculating the G'/G'' ratio, we can determine which applications are more suitable for the CMXn nanocomposites. For frequencies between 0.01 and 10, MXene composites used for

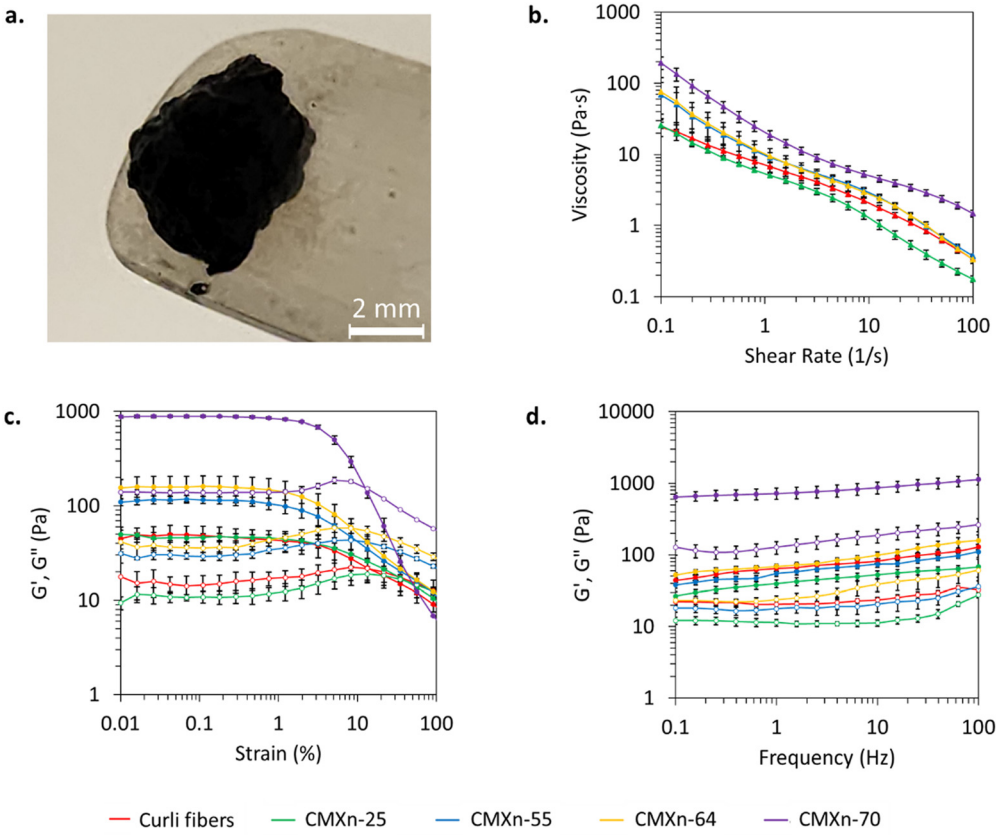

Fig. 3 Rheological properties of CMXn hydrogels. All measurements were done with the nanocomposites in their hydrated state: (a) close-up image of CMXn-70 hydrogel, (b) viscosity as a function of shear rate (solid triangle markers), storage (G') and loss (G'') modulus (solid and empty circles, respectively) under (c) amplitude & (d) frequency sweeps.

extrusion printing applications have reported G'/G'' ratios between 2.5–20.[8] On the other hand, blends between ratios of 2.5–6.0 have been reported for wet spinning applications as well as ratios of 7–20 for dry spinning. The G'/G'' for CMXn hydrogels fall within 2–6 (Fig. S2, ESI†), which shows that the nanocomposites may be suitable for use in wet and dry spinning applications as well.

Lastly, we performed an ultimate tensile test on the fabricated CMXn films to see how MXene loading affected their mechanical properties (stress–strain curves can be seen in Fig. S3, ESI†). To reduce the brittleness of the films, glycerol was added to the nanocomposites, which acted as a plasticizing agent. While there are other plasticizing agents that can be used to provide similar effects, glycerol was used due to its polar and hydrophilic nature. Glycerol has been extensively used for the same purpose in other protein-based films.[40–42] Glycerol has increased the elongation at break 30- and 60-fold by adding 30 and 60 wt% of glycerol in chitosan/zein films and similarly achieved a strain of up to 364% when adding 30 wt% in silk films.[41,42]

CMXn-25 displayed the lowest Young's modulus (4.3 ± 1.1 MPa) and ultimate stress (0.9 ± 0.2 MPa) values and was able to withstand a strain of up to 83.8 ± 21.6% (Fig. 4(b)–(d), respectively). The remaining CMXn films, however, increased Young's modulus by 7–25-fold and ultimate stress by 1.5–5-fold. In contrast, the ultimate strain showed by CMXn-55, -64 and -70 dropped to values between 7–20%. As expected, as MXene loading increased in the CMXn films, their Young's modulus and ultimate stress values would increase while reducing their strain.[17] On the other hand, we also observed that several of the CMXn films showed no significant differences between them. We attribute this to variations such as heterogeneous film thicknesses when preparing the films as well as the samples having featuring "curling" behavior which left the not being completely flattened out. Low MXene loading CMXn films such as CMXn-25 exhibit promising flexible properties (coupled with their conductivity) for a material that may be employed as a strain sensor or for electromagnetic interference (EMI) shielding applications.

Conductivity of CMXn hydrogels

We then characterized the conductivity of the CMXn hydrogels as a function of their MXene loading (Fig. 5(b)). Curli fibers displayed a low conductivity of 1.6 ± 0.5 nS cm^{-1} and marginally increased to 44 ± 12 nS cm^{-1} with a load of 25 wt%, which form part of the insulation region. The conductivity of CMXn-55 increased by 6 orders of magnitude, up to 35 ± 2 mS cm^{-1}, which could represent the start of the conduction region. The conductivity then further increased for CMXn-64 & -70, reaching 22 ± 12 S cm^{-1} and 49 ± 28 S cm^{-1} respectively.

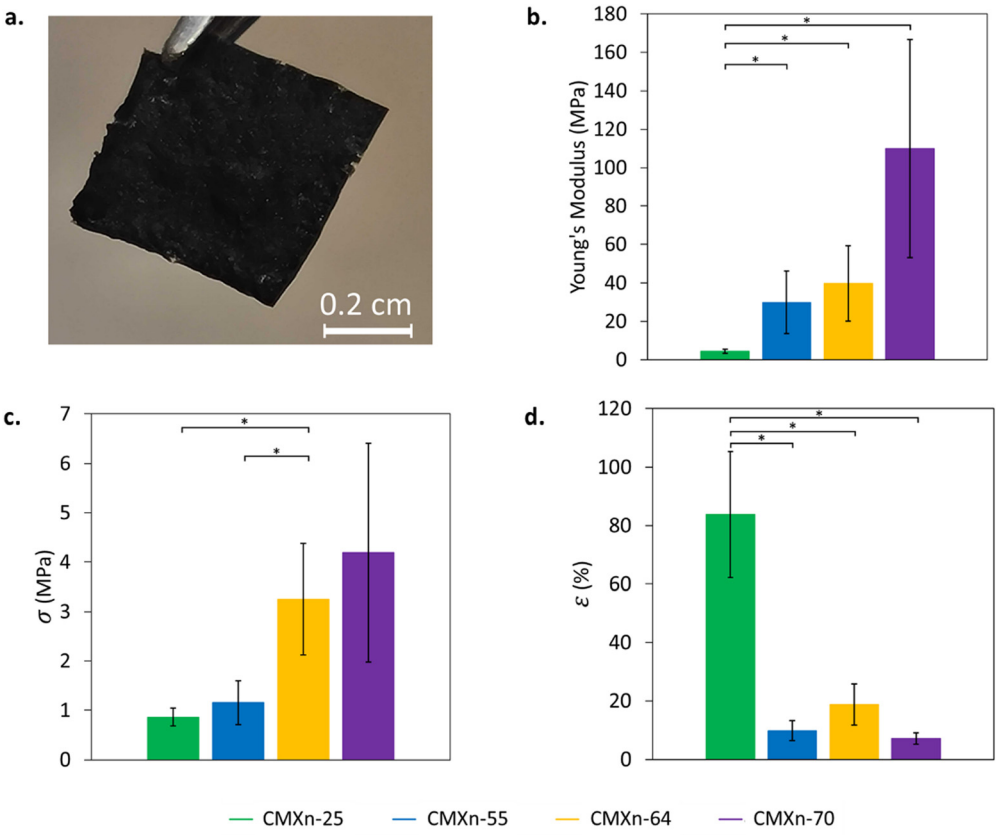

Fig. 4 Mechanical properties of CMXn thin films. Tensile test measurements for dried CMXn films: (a) close-up image of CMXn-55 film with dimensions of 0.5 mm × 0.5 mm, (b) Young's modulus and ultimate (c) stress (σ) & (d) strain (ε). A t-test was applied to determine if the samples were statistically different if lower than *p = 0.05.

The percolation region of MXene loading is thus between 30–50 wt%, a behavior like that observed for other composites containing MXene, with percolation ranges between 1–40 wt% of MXene loads.[10,17,32]

The stability of MXene is an important consideration, as it can have an impact on the shelf life of the nanocomposites. It has been reported that aqueous MXene dispersions degrade in approximately 16 days if left at RT (observing a change in color from black to white and a drop in conductivity) while leaving it at 5 °C increases its shelf life to 5 weeks.[43,44] This is largely attributed to the oxygen present in the solution which reacts with the surface of MXene to form TiO_2 (either anatase and/or rutile), and by decreasing the temperature, the interactions with oxygen and water molecules are reduced.[44] On the other hand, light also plays a role in facilitating the oxidation of MXene.[43] To reduce the likelihood of degradation from these environmental factors, we covered all the CMXn hydrogels in aluminum foil and stored them in the fridge at 4 °C.

By considering that structural changes in MXene are linked to specific environmental conditions which result in conductivity drops, we proceeded to measure the shelf life of CMXn-70 through its conductivity when stored: (1) in the dark at 4 °C (Fig. 5(c), blue) and (2) left exposed to light at RT (Fig. 5(c), red) over a 32-day period. The conductivity of CMXN-70 at 4 °C was stable throughout the entire period, with initial measurements oscillating between 15–40 S cm^{-1} for the first 3 weeks. In comparison, leaving CMXn-70 at room temperature considerably reduced its conductivity, decreasing from an initial value of 10 ± 2.2 S cm^{-1} to 0.25 ± 0.1 S cm^{-1} after 4 days, a 98% decrease. A similar behavior has been reported for MXene–PVA films that showed 7–40% decrease in of their initial conductivities over the course of a month.[45] The CMXn-70 hydrogel was stable when refrigerated but was not the case when left at room temperature, where it showed a 200-fold drop over the first 12 days. The results highlight the impact of storage conditions on the conductivity of CMXn hydrogels.

We then asked ourselves whether curli fibers would have an impact on the stability of MXene over time, and how changes in conductivity of pure MXene would compare with the conductivity of CMXn-70. An aqueous dispersion of MXene was stored at the same set of conditions: (1) in the dark at 4 °C (Fig. 5(d), blue) or (2) exposed to light at RT (Fig. 5(d), red). The conductivity of MXene stored at 4 °C was stable throughout 32 days, showing variations between 1000–3000 S cm^{-1}. On the other hand, the conductivity of MXene left at RT dropped to values between 200–700 S cm^{-1}. While initially stable over 3 weeks, MXene stored at RT displayed a considerable drop in conductivity by day 32, decreasing to 0.2 ± 0.03 S cm^{-1}.

Overall, both CMXn-70 and pure MXene were quite stable when left in the dark at 4 °C, but there was a notable difference

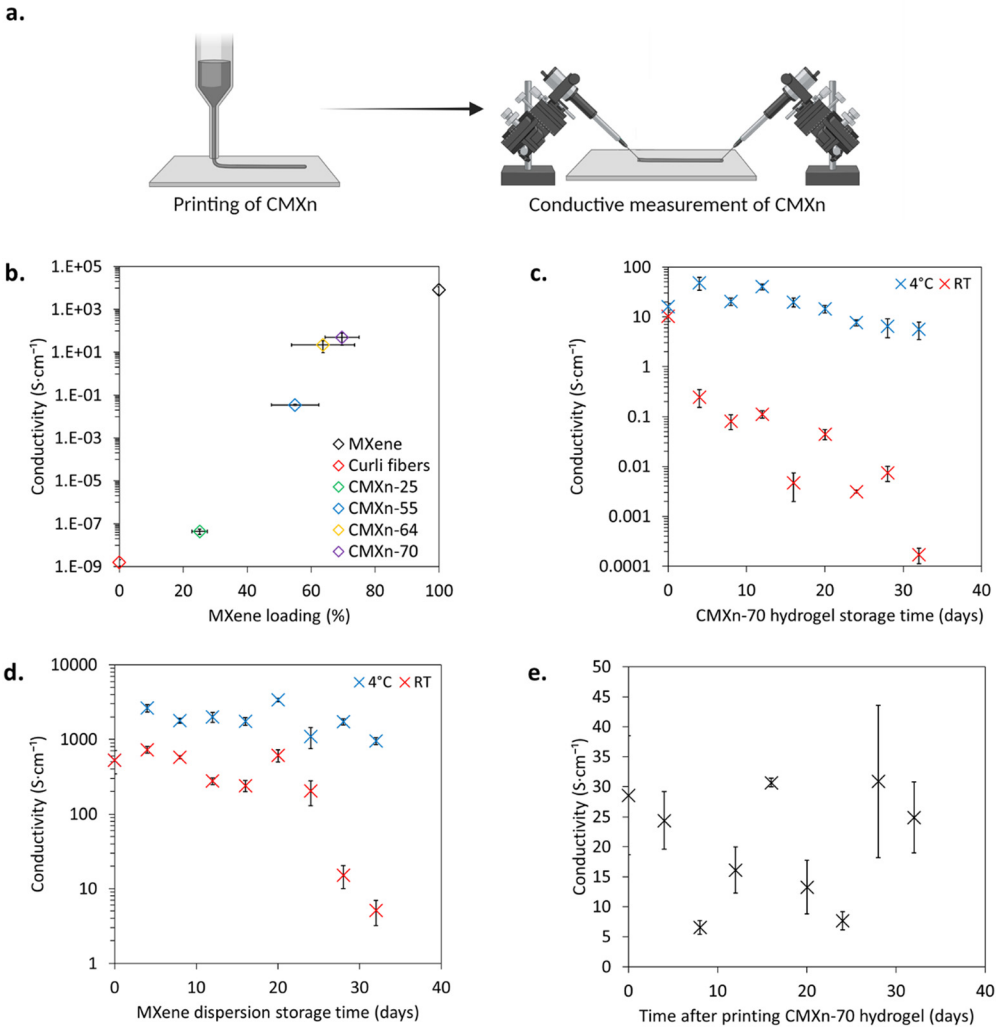

Fig. 5 Conductivity of printed CMXn hydrogels over time. (a) Schematic of conductivity measurements at RT & 45% relative humidity (RH) for printed CMXn hydrogels, followed by (b) conductivity measurements of CMXn hydrogels plotted as a function of their MXene load, (c) shelf life of CMXn-70 hydrogel at refrigerated (4 °C) and RT conditions, (d) shelf life of MXene dispersion at 4 °C and RT & (e) stability of printed CMXn-70 hydrogel.

in their behavior when left exposed to light at RT. We observed a 97% drop in conductivity for CMXn-70 stored at RT in the first 4 days, and its conductivity kept decreasing until reaching a final conductivity of about 0.01% of its original value. In contrast, RT stored MXene showed no major conductivity changes the first 3 weeks, but its conductivity started to decrease down to 97% of its original value by day 28. While MXene eventually showed changes in its structure that caused a drop in conductivity, this did not occur immediately. The substantial drop in conductivity seen in CMXn-70 at RT can be attributed to the presence of curli fibers, as they represent the main difference between the two samples. While further investigations would be required to fully assess how curli fibers change over time within the nanocomposites, we postulate that their viscosity may be decreasing at RT (compared with when they are stored at 4 °C) which may affect the integrity of the CMXn hydrogels and decrease its conductivity.[22] Bacterial contamination (which is unavoidable when using the vacuum filtration process to isolate curli fibers) may also play a role in negatively impairing the conductivity of the CMXn hydrogels, if the bacterial cells proliferate at RT and change the composition of the materials.[20] In addition, MXene is a known reducing agent for several chemical species, and it may also be possible that SDS (traces remaining present in the curli hydrogel after vacuum filtration) along with the amino acid side chains from curli fibers may be reacting with MXene, which would affect its conductivity.[46,47]

Considering how the storage conditions were affecting the stability of CMXn-70 and MXene, we decided to also test the shelf-life of the printed CMXn-70 hydrogel. The CMXn-70 hydrogel was printed and left under ambient conditions, measuring the same samples over a 32-day period at RT & 45% RH. Initially, the conductivity of printed CMXn-70 was 25 ± 6 S cm^{-1} (Fig. 5(e)) and throughout the month, conductivity showed fluctuations between 7–30 S cm^{-1}. As opposed to the bioink in hydrogel form, this trend is indicative that the printed nanocomposite is stable and seems to show minimal signs of degradation over time. There is, however, a noticeable

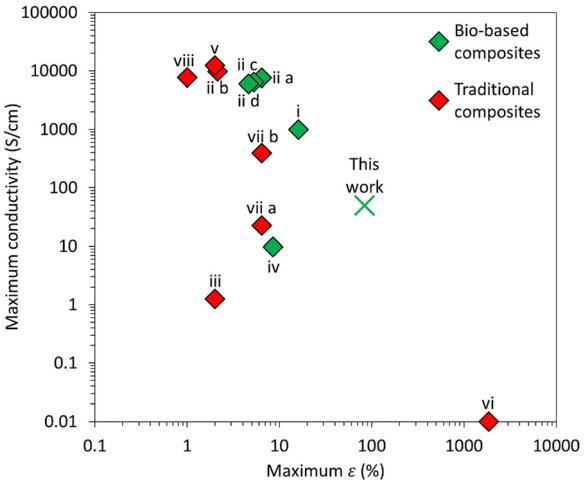

Fig. 6 Comparison of maximum ultimate strain (ε) and maximum conductivity achieved by other MXene composite films using different manufacturing techniques. Nomenclature and numerical values are shown in Table S1 (ESI†). Further mechanical properties and assembly techniques are shown in Table S2 (ESI†).

variability in the measurements which were primarily attributed to small humidity changes between 35–40% that occurred throughout the study and to a lesser extent to small variations in ambient temperature (which was stable between 20–22 °C).

Other bio-based composites with MXene have been generated, with each compound having a different function or integration strategy (Fig. 6). For instance, the use of bacterial cellulose (i) was done to alleviate the restacking of MXene sheets while looking an abundantly available but environmentally safe compound.[48] On the other hand, montmorillonite (MMT) (iii) was used to provide high tensile strength while at the same time taking advantage of its negative charges to employ a layer-by-layer (LBL) assembly with MXene.[49] In similar fashion, the positive charges of chitosan (ii) also facilitated a multilayered composite with MXene through LBL, using a more abundant and biologically derived material.[50] In contrast to these bio-composites, the goal of using curli fibers was to take advantage of their hydrophilic nature and their vacuum filtration purification process to incorporate MXene.

While the conductivity of CMXn hydrogels/films is comparable (though lower) to these composites that have employed bacterial cellulose (i), chitosan (iv) or montmorillonite (MMT)/PVA (iii) with similar MXene loads, ranging from 0.1–1000 S cm^{-1} (Fig. 6), there is a noticeable difference in the strain that they are able to withstand. CMXn films can support up to 84% in contrast to values ranging from 2–16% for other composites. Vacuum filtration processes provide a simple method to incorporate MXene into different materials, having been used to generate MXene-bacterial cellulose (i), hydrogen-bonded MXene-carboxymethyl cellulose (CMC) film (iia), covalently bridged MXene-boron film (iib) or MXene-graphdiyne nanotube (see Table S2, ESI†).[48,51,52] However, composites such as the MXene-CMC or MXene-boron films required prior complex synthesis methods to enhance their stability, rather than simply relying on the vacuum filtration procedure. The use of curli fibers as a biologically derived scaffold for MXene displayed conductivity of up to 50 S cm^{-1} and withstand strains that are at least 5-fold higher than both bio-based and traditionally based composites. Coupled with a simple fabrication method, they show great potential to be used as a strain sensor or alternatively for EMI shielding applications.

Conclusion

In conclusion, we have established a method to load MXene into curli fiber hydrogels, as part of which we can modulate the final content of MXene in the nanocomposites. We have characterized the electrical and mechanical properties of CMXn hydrogels both in hydrated and dried forms and evaluated their suitability for printing and thin film fabrication. The nanocomposites showed noticeable changes in conductivity as a function of the MXene loading. The CMXn hydrogels showed shear thinning properties that were ideal for extrusion printing applications, as demonstrated by the printed bioink traces that we prepared. Similarly, CMXn prepared as thin films showed that they can withstand large strains at break for lower MXene loadings, a property imbued by the curli fiber matrix. To maintain their stability, CMXn hydrogels require to be stored away from light and at 4 °C, but the printed dried nanocomposites were stable and maintained a constant conductivity under ambient conditions for a month. The properties exhibited by CMXn hydrogels are promising for further applications of these materials as strain, humidity, or temperature sensors, as well as for use in flexible electronics. Additionally, the use of curli fibers as a scaffold could allow to further genetically engineer the nanocomposites and introduce new functionalities, such as fluorescence, enzymatic reactions or specific metallic adhesion, all of which may become relevant in interfacing electronics with biological systems.[19]

Author contributions

M. A. A. G. conceptualized the project, designed the protocol to integrate MXene into curli fibers, obtained TGA data, performed rheological measurements, collected SEM and EDS images, gathered conductivity measurements, analyzed the results and wrote the manuscript. S. H. conceptualized the project, performed XRD and FTIR spectroscopy tests and analyzed the results. J. M. L. performed mechanical tests. D. M. obtained profilometry data. X. H. gathered conductivity measurements. P.-Y. C. provided the MAX phase and protocols for MXene synthesis, and supervised the work. N.-M. D. C. conceptualized the project, acquired funding, and supervised the work. All authors contributed to writing – editing the manuscript and have approved its submission.

Data availability

Data for this article is available in Open Science Framework (OSF) at osf.io/yf378.

Conflicts of interest

There are no conflicts to declare.

Acknowledgements

This research was undertaken, in part, thanks to funding from the Canada Research Chairs (CRC) Program (Canada Research Chair in Biologically-Derived Materials awarded to N.-M. D. C.). This work was also supported by the Natural Sciences and Engineering Research Council of Canada (NSERC) through a Discovery Grant (awarded to N.-M. D. C.), by the McGill Sustainability Systems Initiative (MSSI) Ideas Fund (grant awarded to N.-M. D. C.), and by Johnson & Johnson through a WiSTEM2D Scholars Award (awarded to N.-M. D. C.). P.-Y. C. acknowledges the financial support provided by the Start-Up Fund of University of Maryland, College Park (KFS no. 2957431 to P.-Y. C.). Funding for this research was also provided, in part, by MOST-AFOSR Taiwan Topological and Nanostructured Materials Grant under grant no. FA2386-21-1-4065 (KFS no. 5284212 to P.-Y. C.). M. A. A. G. gratefully acknowledges support from NSERC through a Collaborative Research and Training Experience in Sustainable Electronics and Eco-Design (CREATE SEED) Doctoral Scholarship, as well as support from a joint Mexican National Council of Humanities, Sciences and Technologies (CONAHCYT) and Secretariat of Energy (SENER) Energy Sustainability Scholarship. D. M. would like to acknowledge support from Fonds de recherche du Québec – Nature et Technologies (FRQNT) for a Doctoral Research Scholarship, as well as support from the Faculty of Engineering at McGill University for a Vadasz Fellow McGill Engineering Doctoral Award (Vadasz MEDA). X. H. would like to acknowledge support from a McGill Engineering Undergraduate Student Masters Award (MEUSMA). Fig. 1(a) and 5(a) in this document were created using BioRender.com.

References

1 S. Nasiri and M. R. Khosravani, Progress and challenges in fabrication of wearable sensors for health monitoring, *Sens. Actuators, A*, 2020, **312**, 112105.
2 Y. Song, D. Mukasa, H. Zhang and W. Gao, Self-Powered Wearable Biosensors, *Acc. Mater. Res.*, 2021, **2**(3), 184–197.
3 K. Liu, S. Wei, L. Song, H. Liu and T. Wang, Conductive Hydrogels—A Novel Material: Recent Advances and Future Perspectives, *J. Agric. Food Chem.*, 2020, **68**(28), 7269–7280.
4 F. Fu, J. Wang, H. Zeng and J. Yu, Functional Conductive Hydrogels for Bioelectronics, *ACS Mater. Lett.*, 2020, **2**(10), 1287–1301.
5 W. Zhang, P. Feng, J. Chen, Z. Sun and B. Zhao, Electrically conductive hydrogels for flexible energy storage systems, *Prog. Polym. Sci.*, 2019, **88**, 220–240.
6 L. Hao, C. Dong, L. Zhang, K. Zhu and D. Yu, Polypyrrole Nanomaterials: Structure, Preparation and Application, *Polymers*, 2022, **14**(23), 5139.
7 Ö. Yağci and O. K. Özdemir, Improving the electrical conductivity and electrochemical properties of PEDOT:PSS thin films by Ca and Mg doping, *Polym. Bull.*, 2022, **79**(12), 11493–11509.
8 B. Akuzum, K. Maleski, B. Anasori, P. Lelyukh, N. J. Alvarez and E. C. Kumbur, *et al.*, Rheological Characteristics of 2D Titanium Carbide (MXene) Dispersions: A Guide for Processing MXenes, *ACS Nano*, 2018, **12**(3), 2685–2694.
9 T. Zhang, L. Pan, H. Tang, F. Du, Y. Guo and T. Qiu, *et al.*, Synthesis of two-dimensional $Ti_3C_2T_x$ MXene using HCl + LiF etchant: Enhanced exfoliation and delamination, *J. Alloys Compd.*, 2017, **695**, 818–826.
10 Z. Ling, C. E. Ren, M.-Q. Zhao, J. Yang, J. M. Giammarco and J. Qiu, *et al.*, Flexible and conductive MXene films and nanocomposites with high capacitance, *Proc. Natl. Acad. Sci. U. S. A.*, 2014, **111**(47), 16676–16681.
11 L. Chen, X. Shi, N. Yu, X. Zhang, X. Du and J. Lin, Measurement and Analysis of Thermal Conductivity of $Ti_3C_2T_x$ MXene Films, *Materials*, 2018, **11**(9), 1701.
12 K. Rasool, M. Helal, A. Ali, C. E. Ren, Y. Gogotsi and K. A. Mahmoud, Antibacterial Activity of $Ti_3C_2T_x$ MXene, *ACS Nano*, 2016, **10**(3), 3674–3684.
13 Y. Wang, N. Chen, B. Zhou, X. Zhou, B. Pu and J. Bai, *et al.*, NH_3-Induced In Situ Etching Strategy Derived 3D-Interconnected Porous MXene/Carbon Dots Films for High Performance Flexible Supercapacitors, *Nano-Micro Lett.*, 2023, **15**(1), 231.
14 W. Eom, H. Shin, R. B. Ambade, S. H. Lee, K. H. Lee and D. J. Kang, *et al.*, Large-scale wet-spinning of highly electroconductive MXene fibers, *Nat. Commun.*, 2020, **11**(1), 2825.
15 X. Wu, H. Liao, D. Ma, M. Chao, Y. Wang and X. Jia, *et al.*, A wearable, self-adhesive, long-lastingly moist and healable epidermal sensor assembled from conductive MXene nanocomposites, *J. Mater. Chem. C*, 2020, **8**(5), 1788–1795.
16 X. Mi, Z. Su, Y. Fu, S. Li and A. Mo, 3D printing of Ti_3C_2-MXene-incorporated composite scaffolds for accelerated bone regeneration, *Biomed. Mater.*, 2022, **17**(3), 035002.
17 S. Seyedin, S. Uzun, A. Levitt, B. Anasori, G. Dion and Y. Gogotsi, *et al.*, MXene Composite and Coaxial Fibers with High Stretchability and Conductivity for Wearable Strain Sensing Textiles, *Adv. Funct. Mater.*, 2020, **30**(12), 1910504.
18 M. M. Barnhart and M. R. Chapman, Curli Biogenesis and Function, *Annu. Rev. Microbiol.*, 2006, **60**(1), 131–147.
19 P. Q. Nguyen, Z. Botyanszki, P. K. R. Tay and N. S. Joshi, Programmable biofilm-based materials from engineered curli nanofibres, *Nat. Commun.*, 2014, **5**(1), 4945.
20 N.-M. Dorval Courchesne, A. Duraj-Thatte, P. K. R. Tay, P. Q. Nguyen and N. S. Joshi, Scalable Production of Genetically Engineered Nanofibrous Macroscopic Materials via Filtration, *ACS Biomater. Sci. Eng.*, 2017, **3**(5), 733–741.
21 A. M. Duraj-Thatte, A. Manjula-Basavanna, N. M. D. Courchesne, G. I. Cannici, A. Sánchez-Ferrer and B. P. Frank, *et al.*, Water-processable, biodegradable and coatable aquaplastic from engineered biofilms, *Nat. Chem. Biol.*, 2021, **17**(6), 732–738.
22 C. Huyer, D. Modafferi, M. Aminzare, J. Ferraro, Z. Abdali and S. Roy, *et al.*, Fabrication of Curli Fiber-PEDOT:PSS Biomaterials with Tunable Self-Healing, Mechanical, and

Electrical Properties, *ACS Biomater. Sci. Eng.*, 2023, **9**(5), 2156–2169.

23 N.-M. Dorval Courchesne, E. P. DeBenedictis, J. Tresback, J. J. Kim, A. Duraj-Thatte and D. Zanuy, *et al.*, Biomimetic engineering of conductive curli protein films, *Nanotechnology*, 2018, **29**(45), 454002.

24 E. Axpe, A. Duraj-Thatte, Y. Chang, D.-M. Kaimaki, A. Sanchez-Sanchez and H. B. Caliskan, *et al.*, Fabrication of Amyloid Curli Fibers–Alginate Nanocomposite Hydrogels with Enhanced Stiffness, *ACS Biomater. Sci. Eng.*, 2018, **4**(6), 2100–2105.

25 A. M. Duraj-Thatte, A. Manjula-Basavanna, J. Rutledge, J. Xia, S. Hassan and A. Sourlis, *et al.*, Programmable microbial ink for 3D printing of living materials produced from genetically engineered protein nanofibers, *Nat. Commun.*, 2021, **12**(1), 6600.

26 B. Fan, X. Zhao, P. Zhang, Y. Wei, N. Qiao and B. Yang, *et al.*, Effect of Sodium Dodecyl Sulfate on Stability of MXene Aqueous Dispersion, *Adv. Sci.*, 2023, **10**(24), 2300273.

27 J. Dandurand, V. Samouillan, M. H. Lacoste-Ferre, C. Lacabanne, B. Bochicchio and A. Pepe, Conformational and thermal characterization of a synthetic peptidic fragment inspired from human tropoelastin: Signature of the amyloid fibers, *Pathol. Biol.*, 2014, **62**(2), 100–107.

28 M. Seredych, C. E. Shuck, D. Pinto, M. Alhabeb, E. Precetti and G. Deysher, *et al.*, High-Temperature Behavior and Surface Chemistry of Carbide MXenes Studied by Thermal Analysis, *Chem. Mater.*, 2019, **31**(9), 3324–3332.

29 Z. Li, L. Wang, D. Sun, Y. Zhang, B. Liu and Q. Hu, *et al.*, Synthesis and thermal stability of two-dimensional carbide MXene Ti_3C_2, *Mater. Sci. Eng., B*, 2015, **191**, 33–40.

30 Y. Pan, L. Fu, Q. Zhou, Z. Wen, C.-T. Lin and J. Yu, *et al.*, Flammability, thermal stability and mechanical properties of polyvinyl alcohol nanocomposites reinforced with delaminated $Ti_3C_2T_x$ (MXene), *Polym. Compos.*, 2020, **41**(1), 210–218.

31 M. Mahmood, A. Rasheed, I. Ayman, T. Rasheed, S. Munir and S. Ajmal, *et al.*, Synthesis of Ultrathin MnO_2 Nanowire-Intercalated 2D-MXenes for High-Performance Hybrid Supercapacitors, *Energy Fuels*, 2021, **35**(4), 3469–3478.

32 M. Naguib, T. Saito, S. Lai, M. S. Rager, T. Aytug and M. Parans Paranthaman, *et al.*, $Ti_3C_2T_x$ (MXene)–polyacrylamide nanocomposite films, *RSC Adv.*, 2016, **6**(76), 72069–72073.

33 Y.-J. Wan, X.-M. Li, P.-L. Zhu, R. Sun, C.-P. Wong and W.-H. Liao, Lightweight, flexible MXene/polymer film with simultaneously excellent mechanical property and high-performance electromagnetic interference shielding, *Composites, Part A*, 2020, **130**, 105764.

34 M. Aakyiir, H. Yu, S. Araby, W. Ruoyu, A. Michelmore and Q. Meng, *et al.*, Electrically and thermally conductive elastomer by using MXene nanosheets with interface modification, *Chem. Eng. J.*, 2020, **397**, 125439.

35 M. Benchakar, L. Loupias, C. Garnero, T. Bilyk, C. Morais and C. Canaff, *et al.*, One MAX phase, different MXenes: A guideline to understand the crucial role of etching conditions on $Ti_3C_2T_x$ surface chemistry, *Appl. Surf. Sci.*, 2020, **530**, 147209.

36 J. Halim, K. M. Cook, M. Naguib, P. Eklund, Y. Gogotsi and J. Rosen, *et al.*, X-ray photoelectron spectroscopy of select multi-layered transition metal carbides (MXenes), *Appl. Surf. Sci.*, 2016, **362**, 406–417.

37 M. A. Hope, A. C. Forse, K. J. Griffith, M. R. Lukatskaya, M. Ghidiu and Y. Gogotsi, *et al.*, NMR reveals the surface functionalisation of Ti_3C_2 MXene, *Phys. Chem. Chem. Phys.*, 2016, **18**(7), 5099–5102.

38 A. Rozmysłowska, T. Wojciechowski, W. Ziemkowska, L. Chlubny, A. Olszyna and S. Poźniak, *et al.*, Colloidal Properties and Stability of 2D Ti_3C_2 and Ti_2C MXenes in Water, *Int. J. Electrochem. Sci.*, 2018, **13**(11), 10837–10847.

39 E. P. DeBenedictis, J. Liu and S. Keten, Adhesion mechanisms of curli subunit CsgA to abiotic surfaces, *Sci. Adv.*, 2016, **2**(11), e1600998.

40 M. G. A. Vieira, M. A. da Silva, L. O. dos Santos and M. M. Beppu, Natural-based plasticizers and biopolymer films: A review, *Eur. Polym. J.*, 2011, **47**(3), 254–263.

41 H. Lyu, Z. Sun, Y. Liu, X. Yu and C. Guo, Processing-Structure-Properties Relationships of Glycerol-Plasticized Silk Films, *Molecules*, 2022, **27**(4), 1339.

42 Y. Sun, Z. Liu, L. Zhang, X. Wang and L. Li, Effects of plasticizer type and concentration on rheological, physico-mechanical and structural properties of chitosan/zein film, *Int. J. Biol. Macromol.*, 2020, **143**, 334–340.

43 J. Li, R. Qin, L. Yan, Z. Chi, Z. Yu and N. Li, *et al.*, Plasmonic Light Illumination Creates a Channel To Achieve Fast Degradation of $Ti_3C_2T_x$ Nanosheets, *Inorg. Chem.*, 2019, **58**(11), 7285–7294.

44 Y. Chae, S. J. Kim, S.-Y. Cho, J. Choi, K. Maleski and B.-J. Lee, *et al.*, An investigation into the factors governing the oxidation of two-dimensional Ti_3C_2 MXene, *Nanoscale*, 2019, **11**(17), 8387–8393.

45 T. Habib, X. Zhao, S. A. Shah, Y. Chen, W. Sun and H. An, *et al.*, Oxidation stability of $Ti_3C_2T_x$ MXene nanosheets in solvents and composite films, *npj 2D Mater. Appl.*, 2019, **3**(1), 8.

46 J. M. Little, J. Sun, A. Kamali, A. Chen, A. C. Leff and Y. Li, *et al.*, Noble Metal Ion-Directed Assembly of 2D Materials for Heterostructured Catalysts and Metallic Micro-Texturing, *Adv. Funct. Mater.*, 2023, **33**(30), 2215222.

47 F. Zhao, Y. Yao, C. Jiang, Y. Shao, D. Barceló and Y. Ying, *et al.*, Self-reduction bimetallic nanoparticles on ultrathin MXene nanosheets as functional platform for pesticide sensing, *J. Hazard. Mater.*, 2020, **384**, 121358.

48 S. Jiao, A. Zhou, M. Wu and H. Hu, Kirigami Patterning of MXene/Bacterial Cellulose Composite Paper for All-Solid-State Stretchable Micro-Supercapacitor Arrays, *Adv. Sci.*, 2019, **6**(12), 1900529.

49 J. Lipton, G.-M. Weng, M. Alhabeb, K. Maleski, F. Antonio and J. Kong, *et al.*, Mechanically strong and electrically

conductive multilayer MXene nanocomposites, *Nanoscale*, 2019, **11**(42), 20295–20300.

50 Z. Tan, H. Zhao, F. Sun, L. Ran, L. Yi and L. Zhao, *et al.*, Fabrication of Chitosan/MXene multilayered film based on layer-by-layer assembly: Toward enhanced electromagnetic interference shielding and thermal management capacity, *Composites, Part A*, 2022, **155**, 106809.

51 S. Wan, X. Li, Y. Chen, N. Liu, Y. Du and S. Dou, *et al.*, High-strength scalable MXene films through bridging-induced densification, *Science*, 2021, **374**(6563), 96–99.

52 Y. Wang, N. Chen, Y. Liu, X. Zhou, B. Pu and Y. Qing, *et al.*, MXene/Graphdiyne nanotube composite films for Free-Standing and flexible Solid-State supercapacitor, *Chem. Eng. J.*, 2022, **450**, 138398.